Soft Matter

PAPER

View Article Online
View Journal | View Issue

Cite this: *Soft Matter*, 2016, 12, 9509

Formation and relaxation kinetics of starch–particle complexes†

Frida Iselau,*[ab] Tuan Phan Xuan,[c] Gregor Trefalt,[d] Aleksandar Matic,[c] Krister Holmberg[a] and Romain Bordes*[ae]

The formation and relaxation kinetics of starch–particle complexes were investigated in this study. The combination of cationic nanoparticles in suspension and anionic starch in solution gave rise to aggregate formation which was studied by dynamic light scattering, revealing the initial adsorption of the starch molecules on the particle surface. By examining the stability ratio, *W*, it was found that even in the most destabilized state, *i.e.* at charge neutralization, the starch chains had induced steric stabilization to the system. At higher particle and starch concentrations relaxation of the aggregates could be seen, as monitored by a decrease in turbidity with time. This relaxation was evaluated by fitting the data to the Kohlrausch–Williams–Watts function. It was found that irrespective of the starch to particle charge ratio the relaxation time was similar. Moreover, a molecular weight dependence on the relaxation time was found, as well as a more pronounced initial aggregated state for the higher molecular weight starch. This initial aggregate state could be due to bridging flocculation. With time, as the starch chains have relaxed into a final conformation on the particle surface, bridging will be less important and is gradually replaced by patches that will cause patchwise flocculation. After an equilibration time no molecular weight dependence on aggregation could be seen, which confirms the patchwise flocculation mechanism.

Received 8th June 2016,
Accepted 9th November 2016

DOI: 10.1039/c6sm01312k

www.rsc.org/softmatter

Introduction

In applications like paints, water treatment and paper making a combination of charged nanoparticles, such as silica or polystyrene, and polyelectrolytes (PEs) is often employed. The need for understanding the interactions between the particles and the PE has generated a large number of studies of the colloidal behavior of particles when a PE is added to the particle suspension. The main focus has been to understand how the PE adsorption on the particle surfaces will influence the colloidal stability.[1–5]

The electrostatic interaction between a polyelectrolyte and an oppositely charged particle in suspension is the driving force and induces PE adsorption on the particle surface.[6] However, by adsorbing onto a surface the PE reduces its entropy, which is energetically unfavorable. This is often more than compensated for since the PE adsorption induces an ion exchange process where the PE replaces the counterions. The release of many small inorganic ions is entropically very favorable and the total entropy of the system is therefore increased.[7–9]

Possible mechanisms for polyelectrolyte-induced aggregation of colloidal particles of opposite charge are extensively discussed in the literature.[10,11] Charged particles in solution are typically stable due to electrostatic repulsion. If an oppositely charged polyelectrolyte is added to the suspension it adsorbs onto the particles and reduces the magnitude of their surface charge. Further addition of polyelectrolyte can lead to charge neutralization, where the amount of adsorbed polymer is just right to neutralize the charge of the particle. At this point the attractive van der Waals forces will cause aggregation of the particles.[11] The adsorption of the polyelectrolyte will also enhance aggregation due to interaction with the particles and this interaction is often described in the literature as bridging or patchwise flocculation.[11–13] Bridging flocculation relates to the situation when the polymer is attracted to more than one particle, thereby forming a bridge between the particles.[12] This aggregation mechanism is predominant at high particle concentrations for high molecular weight polymers and it is also considered to be the main flocculation mechanism for neutral polymers.[14]

The other aggregation mechanism discussed in the literature is patchwise flocculation,[4,5,13,15–19] for which it is proposed that the charged polymer chains adsorb in patches onto the

[a] *Department of Chemistry and Chemical Engineering, Chalmers University of Technology, 41296 Göteborg, Sweden. E-mail: frida.iselau@chalmers.se*
[b] *Kemira Kemi AB, 44240 Kungälv, Sweden*
[c] *Department of Physics, Chalmers University of Technology, 41296 Göteborg, Sweden*
[d] *Department of Inorganic and Analytical Chemistry, University of Geneva, Switzerland*
[e] *Vinn Excellence Center SuMo Biomaterials, Chalmers University of Technology, 41296 Göteborg, Sweden. E-mail: bordes@chalmers.se*

† Electronic supplementary information (ESI) available. See DOI: 10.1039/c6sm01312k

particle surface due to electrostatic attraction. This adsorption results in a local charge reversal on the particle surface since it now holds patches of opposite charge. This, in turn, can cause electrostatic attraction between patches of reversed charge on some particles and oppositely charged uncovered patches on other particles.

In early studies, turbidity was used to study the rate of flocculation in systems composed of charged particles and oppositely charged polyelectrolytes.[3,13,20] The impact of molecular weight was thoroughly investigated. In order to be able to capture the increase in turbidity with time, the aggregation half-time was adjusted by adjusting the particle concentration, according to Smoluchowski's theory,[21] which was normally used. These studies led to the proposal of an aggregation mechanism through patchwise flocculation for such systems. In recent years dynamic light scattering (DLS) has been the main analytical tool employed to investigate the aggregation behavior and colloidal stability of particle–polyelectrolyte systems. The procedure has been used to study the effect of ionic strength, molecular weight of the PE and pH on the suspension stability.[2,14,15,22,23] Also in these studies the particle and the PE concentrations have been very low in order to remain in the early stages of aggregation where singlets and doublets are dominant. Hence, by using low concentrations of particles in the aggregation experiments the formation of the aggregates can be studied.

In the investigations discussed above it is assumed that the adsorption of the polymer has reached equilibrium before aggregation of the colloidal particles occurs. This means that the polymer diffusion to the surface, attachment at the surface and reorganization occur before the particles collide.[24] This might not always be the case and if the flocculation occurs prior to obtaining equilibrium, it is referred to as ''non-equilibrium flocculation'' (NEF) in the literature.[25,26] During NEF, the time for collision, t_c, is shorter than the time for polymer relaxation t_r. This implies that when particle collision occurs, the adsorbed polymer chain has not rearranged into an equilibrated conformation. The possibility of initial bridging flocculation is discussed in the literature as an effect of a higher particle collision rate compared to the time needed for the adsorbed polymer to relax into an equilibrated conformation on the particle surface. In this transition state bridging of particles by the polymer can occur and result in a bridging flocculation mechanism.[27]

By using higher particle and PE concentrations, comparable to most industrial applications, the turbidity increase with time due to aggregate formation cannot be monitored since according to Smoluchowski theory[21] the time for particle collision at this particle concentration is around 3 ms. However, with a particle concentration that gives a very fast collision time, t_c shorter than t_r, the particles will collide with the polymer chains attached to the surface in a non-equilibrated conformation. This gives the opportunity to study the rate of the PE reorganization on the particle surfaces and to compare the initial adsorption state with the equilibrated aggregation mechanism. This relaxation kinetics is followed both in short (minutes) and long (hours/days) time periods to determine both the initial adsorption state and the long term stability of the formed aggregates.

Latex/PE systems are used for surface hydrophobization of paper, referred to as surface sizing. In this process starch is commonly used in combination with positively or negatively charged latexes less than 100 nm in size. The particle size plays a very important role for this type of application, as a large surface area is beneficial in the drying process. The starch and the latex are normally first blended and then applied on the paper surface at the dry-end of the paper machine.[28,29] The concentration of starch is typically a few percent and the particle concentration is around 0.1 wt%. In a previous paper the aggregation mechanism and the internal structure were described for cationic particles, labelled SP+, combined with an anionic starch.[28] The results from that work regarding the aggregation mechanism, the shape of the polymer when adsorbed onto the cationic particle surface, as well as the selective adsorption of the high molecular weight amylopectin fraction of the starch during aggregation, are discussed in some detail. The SP+ particles that are used in this study are of practical interest in the paper industry.

As stated above, the majority of the studies related to interactions between suspended particles and polyelectrolytes are performed on dilute systems. Many of these studies focus on the initial aggregation rate at different particle to polyelectrolyte ratios and aim at determining the stability ratio, which is defined as $W = k_{fast}/k$, where k_{fast} is the aggregation rate coefficient at the maximum rate of aggregation and k is the aggregation rate coefficient under the studied conditions. The inverse stability ratio represents the likelihood of obtaining a dimer upon collision between two particles. The stability ratio, W, and the electrophoretic mobility as a function of added polyelectrolyte are employed to study how the stability ratio and the electrophoretic mobility are affected by the molecular weight of the PE, an increase in the ionic strength of the solution and changes in pH. Since the aggregate formation has been the focus of these studies, less attention has been dedicated to the aggregation behavior on a long term basis. In the study reported here we examine the interactions between cationic nanoparticles and an anionic PE. The aggregation was studied by a combination of techniques such as DLS, turbidity and small angle X-ray scattering (SAXS) which allowed us to describe the whole aggregation process starting from aggregate formation and determine the change from electrostatic to steric stabilization at maximum aggregation. We also investigate the relaxation kinetics for the formed aggregates with time. SAXS was used to clarify whether the internal structure and the fractal dimension of the aggregates are affected. To our knowledge this is the first time such a comprehensive picture is reported in a single study.

Experimental section

Materials

The starch powders, oxidized regular potato starch and oxidized waxy potato starch, were both from Avebe, The Netherlands, and used as received. To study the early stages of aggregation, polystyrene particles with a radius of 110 nm decorated with

amidine groups, denoted as AL110, were purchased from Invitrogen (Basel, Switzerland). Before use the particles were dialyzed against Milli-Q water (resistivity >18 MΩ) until a conductivity of less than 8×10^{-5} S m^{-1} was reached. For studying the later stages of aggregation and relaxation kinetics the cationic particles, denoted SP+, were synthesized as described in a previous paper.[29] Milli-Q water was used throughout the study. For the particle charge density titrations solutions of 0.001 N polydiallylmethyl ammonium chloride (polyDADMAC) and sodium polyethylene sulphonate (PES-Na) from BTG Instruments AB were used.

Methods

Starch preparation. 3.5 g of starch powder was suspended in 100 mL Milli-Q water under vigorous stirring. The suspension was allowed to boil vigorously for 10 minutes that rendered a clear, slightly pale yellow starch solution. The cooled starch solution was diluted to a final concentration of 3 wt% calculated on dry weight of the starch. Waxy potato starch had a higher solution viscosity compared to the regular potato starch.

Particle charge density titration. Particle charge density titrations were performed using a Particle Charge Detector, CAS Charge Analyzing System (AFG, Analytic GMBH). This instrument employs an electrokinetic technique where the charge distribution is determined by measuring the streaming potential.[30,31] The sample was titrated with a titrant carrying the opposite charge and the amount of titrant required for charge neutralization at a macroscopic level was used for calculating the charge ratio expressed as μeq per g, where eq stands for equivalents. The samples were filtered using a 0.2 μm hydrophilic syringe filter (Sartorius) before measurement. A charge titration of the SP+ particles with the anionic starch as the titrant was performed in order to investigate the starch to SP+ ratio at charge neutralization.

Dynamic light scattering, DLS. A multiangle light scattering instrument, ALV/CGS-8F, was employed for the dynamic light scattering measurements on the SP+ particles and the SP+/starch aggregates. The instrument was equipped with a solid state laser source of 150 mW and a wavelength λ = 532 nm. The temperature was controlled by a thermostat bath to within ±0.2 °C. The angles of observation (Θ) for the measurements were between 12 and 155 degrees. The intensity autocorrelation function measured by DLS is related to the normalized electric field correlation function, $g_1(t)$, by the Siegert relation.[32] In dilute solutions the relaxation is caused by self-diffusion of the particles and hence the $g_1(t)$ was analyzed in terms of the distribution of relaxation times. Using the Stokes–Einstein equation the hydrodynamic radius (R_H) was calculated from the average diffusion coefficient.

Study of the aggregation behaviour

Aggregation monitoring by DLS. Early stages of aggregation of AL110 particles as a function of starch concentration were studied using an ALV/CGS-8F goniometer. The samples were prepared by mixing appropriate amounts of stock suspension of 0.02 wt% of AL110 particles with 0.005 wt% of starch solution. The background electrolyte concentration was adjusted by adding aqueous NaCl solution. The final concentration of particles in the mixture was kept at 0.00072 wt%. Immediately after mixing, the hydrodynamic radius *vs.* time was monitored with the DLS, where R_H was calculated from the second order cumulant fit. The apparent aggregation rate coefficient k_{app} is then determined from the slope and intersect of the radius *vs.* time curve, for details see the article of Oncsik *et al.*[33] Finally the stability ratio W was calculated by comparing the actual apparent aggregation rate coefficient with the one measured in 930 mM NaCl without added starch, k_{fast}, namely $W = k_{fast}/k_{app}$.

For the simultaneous aggregation and relaxation measurements of the cationic particle suspension in combination with the anionic starch the SP+ concentration was 0.001 wt% and starch corresponding to 1 : 1 in the charge ratio was added to the particle suspension. Both SP+ and starch were filtered using a 0.2 μm hydrophilic syringe filter before mixing.

Aggregate growth monitoring and relaxation

Turbidity. The turbidity measurements were performed on an Agilent Cary 60 UV/Vis instrument and a HP8453 UV/Vis instrument using a quartz cuvette or disposable acrylic cuvettes. The baseline was recorded in Milli-Q water. The value of the absorbance at 400 nm was used as a measure of the turbidity. The particle suspension, 0.1 wt%, was filtered using a 0.2 μm hydrophilic syringe filter (Sartorius) before 2 mL sample was transferred to the cuvette. The starch solution was also filtered using a 0.2 μm hydrophilic syringe filter (Sartorius) before being added to the particle suspension. The starch titrations were carried out as follows. To 2 mL sample in a cuvette aliquots of a 3 wt% starch solution were successively added. After the starch addition the cuvette was shaken vigorously before being put into the instrument for measurements. For the relaxation kinetics study, eight samples, with different amounts of starch added to the particle suspension, were measured simultaneously for a long period of time. The turbidity measurements at an elevated temperature were done using the HP8453 UV/Vis instrument that was equipped with a temperature controlled sample holder. To avoid cooling the sample by the addition of starch, the starch solution was preheated in a water bath. By adding the particle suspension to the starch solution the importance of the order of addition was assessed.

SAXS. Small angle X-ray scattering (SAXS) experiments were carried out at the I911-4 beamline of the MAX-IV laboratory synchrotron.[34] The wavelength used was 0.91 Å. The samples were analyzed in capillaries maintained at 20 °C and were prepared right before the measurements. The samples were prepared by adding different amounts of the 3 wt% starch solution to samples of 2 mL of a 0.1 wt% SP+ suspension. In the SAXS study regular starch was used. Before the measurements both the particle suspension and the starch solution were filtered using a 0.2 μm hydrophilic syringe filter (Sartorius). The scattering of pure solvent (Milli-Q water) was measured. Two-dimensional SAXS images were recorded using a PILATUS 1 M detector (Dectris) with an exposure time of 120 s. The scattering vector q is described by $q = 4\pi \sin\theta/\lambda$, where λ is the wavelength and 2θ is the scattering angle and it was calibrated

with a silver behenate sample. The difference in the radial averaged SAXS 2D images from the sample and the solvent is reported as scattering profiles $I(q)$. Data reduction was processed using the Nika package on Igor pro.[35]

SEC-MALS/RI. A size exclusion chromatography system with a Multiple Angle Light Scattering and Refractive Index (SEC-MALS/RI) detector from Wyatt Technology was used for molecular weight determination. An Optilab T-rEX RI detector and a Dawn Heleos-II MALS detector were used.

Sample injections were done with a Waters 717 plus Autosampler and an in-line degasser from Waters for the mobile phase was used. The separation column, a TSKgel GMPWXL from Tosch Bioscience, had a particle size of 13.0 μm and the dimension of 7.8 mm × 30.0 cm. The mobile phase was 10 mM NaCl + 0.02 wt% NaN_3 and it was filtered and degassed before use. The flow rate was 0.5 mL min^{-1} and the elution time was 30 min. The mobile phase was used as a blank and a Pullulan standard was used for quality control. Triple injections of the samples were done. The starch samples were diluted with Milli-Q water to 2 mg mL^{-1} before analysis. The dn/dc value was set to 0.151 according to the literature.[36]

Electrophoretic mobility and ζ potential. The electrophoretic mobility was measured using a Malvern Nano instrument and disposable measuring cells. The value of the ζ potential was calculated using in-built software that employs similar models as used for phase analysis light scattering.[37] For the electrophoretic mobility measurements on the SP+ suspension, a sample was prepared by diluting the particle suspension to a concentration of 0.05 wt%. Before measurement the sample was filtered using a 0.2 μm hydrophilic syringe filter (Sartorius). For the electrophoretic mobility measurements on the SP+ suspension in combination with the anionic starch the SP+ concentration was 0.1 wt% and a 3 wt% starch solution was added in different amounts to the particle suspension. Both the SP+ and the starch were filtered using the 0.2 μm hydrophilic syringe filter before mixing. The samples were analysed 5 min after the addition of the starch aliquot. No background electrolyte was used. Throughout the titration the pH remained constant around 4.0. A similar procedure was used for the AL110 particles, with the exception that the particle concentration was kept much lower, at 0.00072 wt%.

Results and discussion

System characterization and charge ratio determination of the particle–PE system

In the studied system two types of cationic particles were used in combination with oxidized starch. Starch consists of two types of anhydroglucose chains, amylose and amylopectin. Amylose is a short, linear polymer, while amylopectin has much higher molecular weight and is also highly branched. The ratio between amylose and amylopectin in native starch depends on the source of origin. Regular potato starch contains 20 wt% amylose and 80 wt% amylopectin[38] while waxy potato starch consists of 99 wt% amylopectin. Both regular and waxy potato starch are used in this study. Native starch is often oxidized in order to decrease the molecular weight and thereby also decreases the solution viscosity. Further details of the starch oxidation are given in a previous paper.[39]

Table 1 Starch properties

Sample	M_n (kD)	M_w (kD)	M_w/M_n	Charge density (μeq per g)
Regular starch	202	870	4.3	−176
Waxy starch	1380	3090	2.2	−127

The reason for including both regular and waxy starch in this study relies on previous results.[39] Based on SEC and SAXS data, we concluded that mainly amylopectin participated in the aggregation with the cationic particles.

The charge density was determined by the streaming potential (see Table 1) and the difference in charge density originates from different degree of oxidation.

The starches used in this study were characterized by size exclusion chromatography (SEC).[40] The results of the SEC analysis are listed in Table 1. Waxy starch has a higher weight average molecular weight compared to the regular starch. The polydispersity index, M_w/M_n, for regular potato starch is higher compared to waxy starch.

The SP+ particles consist of a hydrophobic core of the styrene–acrylate copolymer. Colloidal stability is achieved by a cationic stabilizer which is a copolymer of styrene and a quaternary ammonium monomer[29] rendering the particles cationic over a wide pH range. SP+ has a hydrodynamic radius of 22 nm and a ζ potential of +53 mV.

In order to study the aggregate formation by DLS in the early stage for the SP+ particles and starch and extract the stability ratio for the system it is crucial that the collision rate of the particles is low enough to allow capturing the early stage of aggregation. Such measurements with small particles can be challenging because to ensure enough scattering signal one has to increase the concentration of the particles and this increases the collision rate.

With the SP+ particles system, it was found that the collision rate was too high to capture in detail the early stages of aggregation. This is due to the relatively small hydrodynamic radius of the SP+ particles. Therefore, another type of cationic particles, amidine particles with a R_H of 110 nm, AL110, was employed for this part of the study. A comparative analysis of the two particle types was done to support the use of the amidine particles as a model for the SP+ particles. The amidine particles had a ζ potential of +40 mV and the colloidal charge was +17 μeq per g as determined by PCD. The starch to particle charge ratio for the amidine particles and the regular starch can be estimated to be 10 : 1 taken from the charge density titrations.

For the SP+ particles the starch to particle charge ratio could not be obtained in the same straightforward manner since the higher charge density for the SP+ particles and the smaller size lead to fast aggregation. This is known to have a pronounced effect on the reliability of the results from the charge density titration. Therefore, the charge ratio for starch and SP+ was

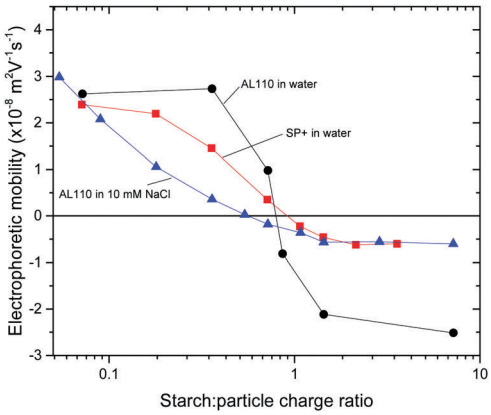

Fig. 1 Plot of electrophoretic mobility *versus* starch : particle charge ratio for amidine particles and SP+ particles. Regular starch was used in this part of the study.

determined by using the starch as a titrant for the SP+ particles and by monitoring the amount of starch needed for charge neutralization of the SP+ particles. This value is then taken as the 1 : 1 charge ratio for the starch : SP+ system.

To a 6 ppm amidine particle suspension different amounts of starch were added and the electrophoretic mobility was monitored. The results are shown in Fig. 1 where electrophoretic mobility is plotted *versus* starch to particle charge ratio. The positive electrophoretic mobility for the AL110 particles decreases with increasing starch to particle ratio and the electrophoretic mobility crosses zero at a starch to particle charge ratio close to 1.

Above 1 : 1 charge ratio, *i.e.* with excess starch, the electrophoretic mobility levels out at a slightly negative value, -2.5×10^{-8} m^2 V^{-1} s^{-1}. This is in accordance with the changes in the electrophoretic mobility for the SP+ particles when starch is added, also shown in Fig. 1.

With increasing amount of starch added to the SP+ particles, the electrophoretic mobility decreases and crosses zero at a starch concentration corresponding to 1 : 1 in the charge ratio. It then levels out at a slightly negative electrophoretic mobility, -0.6×10^{-8} m^2 V^{-1} s^{-1}. This behaviour validates the use of larger amidine particles as a model system for the aggregate formation of the SP+ particles and starch.

Aggregation behavior: kinetics and mechanism

The general aspects of turbidity evolution for the SP+ particle suspension in the presence of starch were discussed in a previous paper.[39] Briefly it can be stated that the addition of starch induced a dramatic increase in turbidity due to the formation of aggregates in the system. The turbidity increased to a maximum at a starch to SP+ charge ratio of around 1. Further addition of starch partially restored the stability of the dispersion, as is evident from the decrease in turbidity above this charge ratio. However, the turbidity did not return to the initial absorbance value observed for the primary SP+ particles, indicating that even in the presence of excess starch, there were still aggregates in the suspension. This was found to be the result of a shift of the stabilization mechanism from electrostatic to electrosteric due to the highly branched amylopectin adsorbed onto the particle surface. Further studies of the aggregation revealed that the initial turbidity was higher compared to the turbidity after an equilibration time. The present study originates form this observation.

DLS was employed to study the formation of the aggregates by the addition of starch. A model system of amidine particles, 110 nm in radius and +40 mV ζ potential, was used to reach sufficient scattering intensity, as the particle concentration to be used with SP+ particles gave rise to a too high collision rate, in order to be able to capture the early stage of aggregation. For larger amidine particles the collision rate was lower and therefore the aggregate formation when starch is added could be monitored. From this DLS study the stability ratio, W, was determined.

The change in turbidity was monitored with time at different starch to SP+ particle charge ratios and from the results the relaxation rates could be obtained. This was done at different particle concentrations, different temperatures, different addition orders as well as different molecular weights of the PE (namely the use of regular and waxy starch).

Complementary experiments were done to follow the aggregate formation, as well as the subsequent relaxation.

Furthermore, the inner aggregate structure was studied by SAXS.

Aggregate formation at the early stages of aggregation. As explained above, for the study of early stages of aggregation in the presence of regular potato starch AL110 particles were used. The aggregation was tracked by DLS by measuring the hydrodynamic radius as a function of time, see Fig. 2a. Experiments were done in 10 mM NaCl solution, to promote aggregation. At low starch to particle charge ratio the aggregation is slow and one can see only a small increase of the hydrodynamic radius with time. Increasing the concentration of starch to particle charge ratio to close to 1 leads to an increase of the slope, *i.e.* the aggregation rate increases. After further addition of starch the slope of the curve decreases again. A comparison of the curves at 0.09 and 2.9 starch to particle charge ratios reveals that the latter curve is shifted by approximately 10 nm. This suggests that at high concentrations of starch the starch layer adsorbed onto the particles is about 10 nm thick. Additionally, one can observe that the rate of increase of the hydrodynamic radius in the presence of starch is much smaller compared to the sample containing only 930 mM NaCl. In the latter situation the aggregation is fast – diffusion controlled. At high salt concentrations the charge of the particles is completely screened and van der Waals attractive forces are dominant. This means that the dimer is formed upon every collision of two single particles.[33] On the other hand, in the presence of starch the aggregation rate is always lower. The quantitative description of the kinetics of the aggregation can be given by presenting the stability ratios, see Fig. 2b. For calculation of stability ratios the fast rate in 930 mM NaCl without addition of starch was used. Therefore the presented results show the stability of suspensions with starch compared to the stability of particles in 930 mM NaCl. The suspensions are stable at low starch

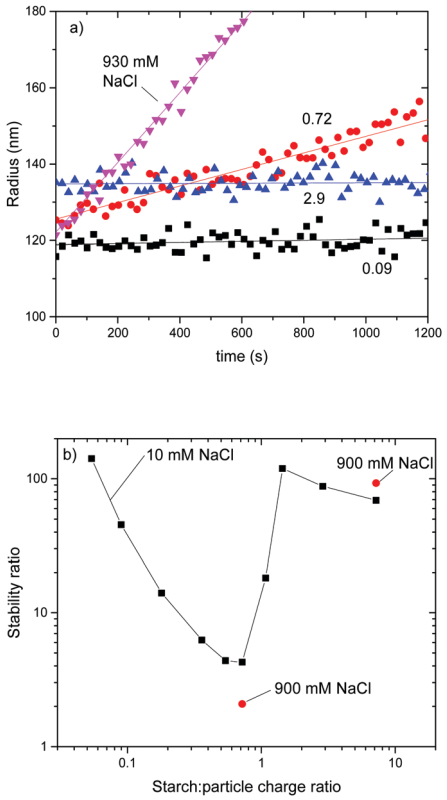

Fig. 2 Aggregation of AL110 particles with regular starch. (a) Time evolution of hydrodynamic radius. Curves for starch to particle charge ratios of 0.09, 0.72 and 2.9 with added 10 mM NaCl as a background salt are shown, as well as the curve in 930 mM NaCl without added starch. (b) Stability ratio as a function of starch to particle charge ratio. 10 mM NaCl background was used (black squares). Two points with 900 mM background NaCl are also presented.

concentrations where the particles are positively charged, as evident from electrophoresis (Fig. 1). At higher concentrations starch neutralizes the particles and the stability ratios have a minimum at about a starch to particle charge ratio of 1. At this point the particles are completely neutralized and they aggregate. Further addition of starch leads to an increased stabilization which plateaus at starch to particle charge ratios above 2. The restablilization could be partly explained by overcharging of the particles, which become negatively charged and again start to repel each other. However, the overcharging is very moderate and it is unlikely that it alone would lead to such a restabilization. It is likely that additional forces such as steric repulsion contribute to the stabilization. Aggregation *via* bridging may not be completely ruled out, however. To address the issue of steric stabilization we did measurements with 900 mM background electrolyte. At this salt level the electrostatic repulsion is completely screened. At the starch to particle charge ratio of about 1, the stability can be further decreased by addition of 900 mM NaCl, however the stability ratio still did not reach the value of 1. A value of the stability ratio at charge neutralization larger than 1 suggests that steric forces induce additional stabilization. At high starch concentration addition of high levels of salt does not affect the stability, which suggests that under these conditions steric stabilization is dominant. Aggregation at a starch to particle charge ratio of around 1 is therefore probably caused by neutralization of particles; however, there may also be contributions of steric stabilization and possibly also patchwise and bridging flocculation.

Aggregate growth and relaxation kinetics. The extent of aggregate formation for the SP+ particles at different PE concentrations was monitored by measuring the change with time of the turbidity for different starch to SP+ charge ratios.

The initial and the equilibrated (after 6 h) turbidity values, for both regular and waxy starch, are shown in Fig. 3. In this figure it can be seen that the shape of the turbidity curve over the whole range of the starch to SP+ charge ratio used in this study is the same for the initial values as for the equilibrated values; the curves differ only in intensity. The maximum turbidity is observed at a starch to SP+ charge ratio of 1, which is in line with the early stage aggregation studies. The large difference in intensity between waxy and regular starch is particularly striking, the initial turbidity for waxy starch being much higher. The aggregation mechanism that was presented in a previous paper[39] concluded that even if the possibility of amylose first adsorbing onto the particles followed by an exchange of amylose by amylopectin may be considered, it was mainly the amylopectin fraction of the starch that participated in the aggregation with the SP+ particles. The higher amount of amylopectin, 99 wt%, compared to 80 wt% for waxy starch, cannot be the sole explanation, since this would only cause a shift in the position of the maximum. Two factors that might contribute to this effect are the presence of amylose that could have an inhibiting effect on the aggregation and the long amylopectin chains in waxy starch that can form aggregates that would require longer rearrangement times.

The SP+ particle concentration of 0.1 wt% that was mainly used in this study is high compared to previous studies using turbidity as a measure of aggregation. A starch titration experiment was also performed where the SP+ particle concentration was 0.05 wt%. When comparing the turbidity curves for the two particle concentrations (Fig. 4), two main differences can be distinguished. First, the magnitude of the turbidity increase is more pronounced for the higher particle concentration. This is expected as more aggregation can take place for the same

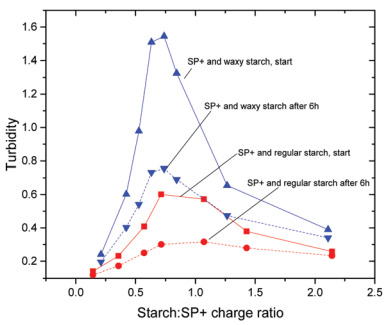

Fig. 3 Initial and equilibrated turbidity curves for the SP+ particles with regular and waxy starch. The turbidity is measured as absorbance at 400 nm.

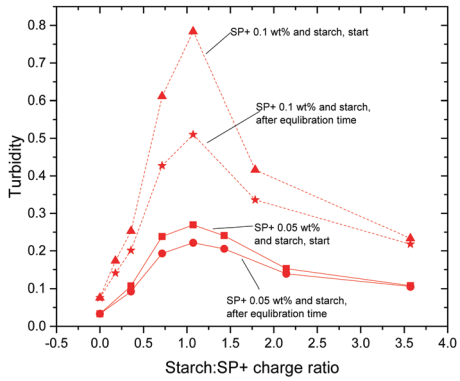

Fig. 4 Turbidity curves for two different SP+ particle concentrations, 0.05 wt% and 0.1 wt%, when combined with regular starch. The highest SP+ particle concentration gives the highest turbidity increase. The initial turbidity increase is more pronounced for the highest particle concentration.

starch to SP+ ratio when more particles are present in the suspension. The second observation is that the initial kinetic contribution to the turbidity increase is higher for the particle concentration of 0.1 wt% compared to that of 0.05 wt%. This is seen from the difference between the initial and the final turbidity values being larger for higher particle concentration.

When the particle concentration is doubled, the time for collision, τ, should be halved according to the Smoluchowski relation $\tau \approx (2 \times 10^{11}/\nu_0)$ seconds, where the particle concentration ν_0 is in particles per cm^3. This means that the collision rate, r_c, is higher at the higher particle concentration and that non-equilibrium flocculation can take place to a larger extent.[20,26] The explanation for this is that the higher the particle concentration, the higher is the probability for the starch chains to interact with more than one particle through bridging flocculation. Initially the starch chains have the possibility to interact with more than one particle surface but rearrangement occurs, giving rise to starch patches on the particles and the aggregation mechanism will then move towards patchwise aggregation,[24,41] which leads to a decrease in turbidity with time. This is in agreement with the discussions in the literature about an initial aggregation state that with time will evolve into an equilibrated aggregation state.[3,20,42] The possibility of initial bridging flocculation is discussed in the literature as an effect of higher particle collision rate compared to the time needed for the adsorbed polymer to relax into an equilibrated conformation on the particle surface. In this transition state bridging of the polymer between particles can occur and result in an initial bridging flocculation.[27]

These results also explain why relaxation could not be seen in the light scattering experiments, wherein the aggregate formation was captured. In that case the very dilute particle and starch system mainly allowed doublets to form and therefore bridging flocculation was unlikely to occur. Furthermore, doublets constitute a form of aggregates that cannot evolve into a more compact form, in the sense that doublets constitute the simplest form of aggregates. Singlets are primary particles that cannot be referred to as aggregates.

The influence of temperature on the aggregation was investigated. First, the temperature impact on the particle suspension and the starch solution alone was addressed by monitoring the turbidity of a 0.1 wt% suspension of SP+ and of a 3 wt% regular starch solution while increasing the temperature. No turbidity change was noted on either system.

For the combination of SP+ and starch a temperature effect on the turbidity could be seen. In the ESI† the turbidity curves for SP+ and starch are plotted for three different temperatures; room temperature, 40 °C and 60 °C. The shape of the curves is the same irrespective of the measuring temperature, but the intensity of the turbidity differs.

There is a decrease in the turbidity maximum with increasing temperature and the plot of turbidity *versus* $1/T$ shows a linear relationship, see Fig. S2 in the ESI.† When comparing the titration curve recorded at 60 °C and the curve for the equilibrated values at room temperature there is good agreement of the values, as seen in Fig. S3 (ESI†). This is reasonable since the system is more dynamic at higher temperatures, which leads to a faster reorganization of the PE chains from bridges to patches on the particle surfaces.

This demonstrates that the relaxation rate after aggregate formation can be accelerated by increased temperature, but in the end the remaining, stable, aggregates will be the same.

By monitoring the variation of turbidity with time the kinetic pattern could be analysed. Starting from the moment when starch was added to the 0.1 wt% SP+ suspension, the turbidity decreases for the whole starch to SP+ charge ratio range included in this study (Fig. 5). Moreover, the decrease was more pronounced the higher the initial turbidity. This means that the charge ratios that resulted in the strongest aggregation also had the largest time dependence in terms of turbidity decrease. Similar behaviour was also observed for waxy starch.

When the data for the different starch to particle ratios were normalized the effect of the different ratios could no longer be seen, as is shown in Fig. S4 in the ESI.† However, an important difference could be seen between the two different starch types (Fig. 6); regular starch had a steeper turbidity decline than waxy starch. This relaxation behaviour of the turbidity with time was evaluated further by fitting the experimental data with the Kohlrausch–Williams–Watts (KWW) relaxation function.

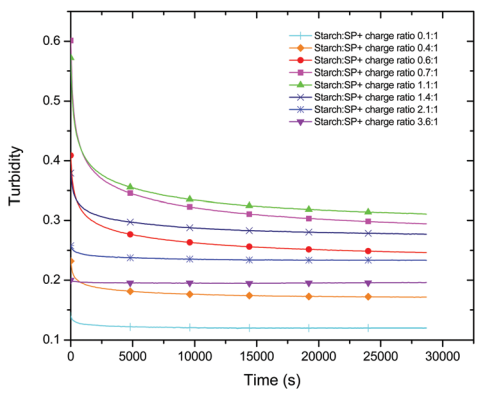

Fig. 5 Turbidity curves as a function of time for different starch (regular) to particle charge ratios.

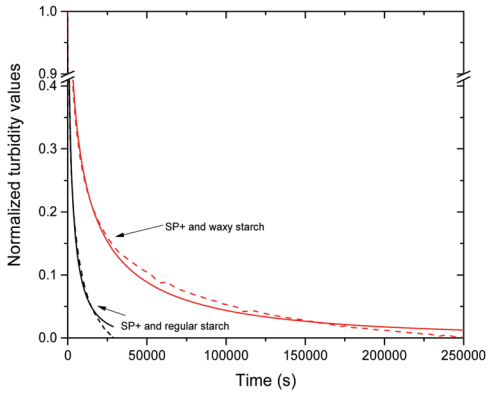

Fig. 6 Normalized kinetic data for the turbidity curves. For simplicity, one curve (dashed lines) for each starch type is shown in the figure together with the fitting of the KWW function (solid lines). Note the break in the curve.

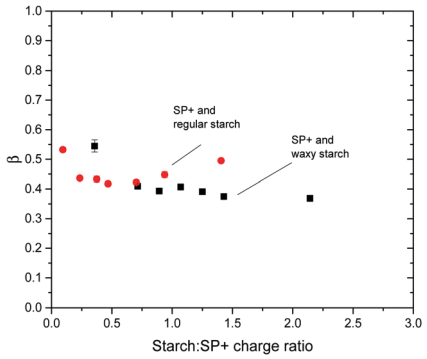

Fig. 7 Plot of relaxation distribution parameter β *versus* starch to particle charge ratio for the combination of SP+ particles and the two different starch types, regular and waxy starch.

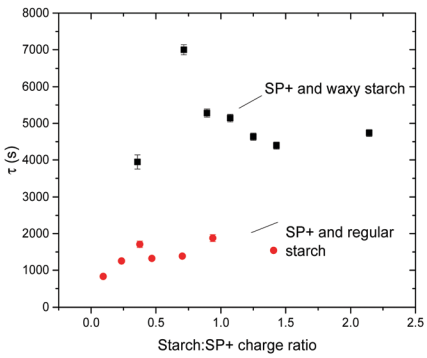

Fig. 8 Plot of relaxation time, τ, *versus* starch to particle charge ratio for the combination of SP+ particles and the two different starch types, regular and waxy starch.

The Kohlrausch–William–Watts function is a stretched exponential function that originates from Kohlrausch's work from 1866,[43] which was further developed by William and Watts.[44] This function is used to describe various types of relaxation data. Historically the focus has been on dielectric relaxation but nowadays it is also used for enthalpy relaxation, light scattering,[45] as well as investigations of polymer solutions[46] and protein aggregation.[47] It is even used as an universal tool for studying various physical and chemical processes.[48]

The KWW function is expressed as

$$y(t) = e^{\left(-\frac{t}{\tau}\right)^{\beta}} \quad (1)$$

where y is the relaxation function expressing the kinetics of the transformation of a non-equilibrium state into an equilibrium state,[49] τ the mean relaxation time, and β the relaxation distribution parameter, which describes how the relaxation deviates from exponential behavior.[47,49] The parameter τ can be seen as a description of the range of relaxation times where most of the relaxation processes take place.[50] The β value can vary between 0 and 1, and when β = 1, the KWW relaxation function becomes exponential. The β parameter can also be seen as a measure of the heterogeneity of the relaxation process. If β is close to 1, the relaxation process is regarded as homogeneous.[51]

The aggregate relaxation data from the turbidity studies of the mixtures of SP+ particles and starch were fitted with the KWW function (1) and from the fitting the relaxation time, τ, and the relaxation distribution parameter, β, were obtained.

The R^2 value for the fitting was >0.95 for all turbidity curves examined with the KWW function. The plots of β and τ *versus* time are shown in Fig. 7 and 8, respectively. The plot of β *versus* time in Fig. 7 shows the similarity between the two starch types regarding the β values. This is especially important as large discrepancies in the β value would not allow the comparisons of the relaxation time between waxy and regular starch.[52] Irrespective of the amount of starch added to the SP+ particle suspension and of the starch type, the β value is around 0.4, supporting a relatively heterogeneous system, as would be expected for a system where multiple reorganization events of the same nature, *i.e.* aggregate structure changes, occur simultaneously.

The τ values for different starch to SP+ charge ratios show no obvious trend, especially in relation to the ratio giving maximum turbidity. This implies that irrespective of the starch to particle charge ratio and the net charge of the complex (as determined by electrophoresis), the time for going from an initial aggregated state to the relaxed equilibrated state where the starch chains have had sufficient time to rearrange on the particle surface is the same.

The magnitude of the turbidity change is evidently affected by the amount of starch added; the maximum turbidity corresponds to a specific starch concentration where the particle suspension is in its most destabilized state. However, it is interesting to note the difference between waxy and regular starch. On average the relaxation time for regular starch is around 1400 s and for waxy starch it is around 4800 s. The fact that waxy starch, which has three times higher M_w than regular starch, also has three times longer relaxation time supports the view that there is an initial aggregation state where bridging flocculation occurs while the equilibrated aggregation is *via* patchwise flocculation. The fact that the relaxation is more pronounced with amylopectin-rich waxy starch than with regular

starch indicates that exchange of amylose by amylopectin does not contribute to the relaxation process.

The relaxation time can also be affected by the strength of the surface attraction.[53] Since regular starch carries a higher anionic charge compared to waxy starch regular starch can be expected to have stronger attraction to the cationic particle surface. This might also contribute to the difference in relaxation time between regular and waxy starch.

After two weeks of storage at room temperature the turbidity of the SP+ particles together with regular starch remains at the same level as presented above, however, the samples with SP+ and waxy starch have dropped considerably in turbidity. No sedimentation was observed that could explain the decreased turbidity. This means that the kinetics for waxy starch when going from bridging flocculation to patchwise flocculation was not entirely captured within the six hours of the study.

SAXS measurements attempted to capture the relaxation kinetics. A SAXS study was performed in order to investigate whether the inner structures of the formed aggregates are affected by the relaxation process. The time for sample preparation and the actual scattering measurements did not allow us to capture the aggregation as early as in the turbidity measurements; the first time point is approximately three minutes after mixing, during this time some relaxation may already have occurred. The scattering intensity for each sample was monitored for one hour. The SAXS data, plotted in a log–log diagram of $I(q)$ *vs.* q are shown in Fig. S5 in the ESI.† In the log–log diagram the two regimes correspond to two structure levels, the first one belonging to the cationic particles with adsorbed starch and, at higher q values, the second one belonging to the adsorbed starch, as discussed in a previous paper.[39] The fractal dimensions, determined from the slope, were in the range of 2.6–4.0, depending on the starch to particle ratio.

No change in intensity over time could be seen for any of the different starch to particle ratios.

In a paper by Cosgrove *et al.* from 1981,[54] it is argued that the hydrodynamic radius ''is determined by the very longest tails'', which can be less than 5% of the total amount, *i.e.* the long tails contribute much to R_H and to the initial bridging flocculation. However, from the SAXS data the radius of gyration, R_G, and not the R_H, is obtained and that could be the reason for no visible change of the inner structure or fractality with time.

Simultaneous aggregation and relaxation measurements. The finding from the turbidity study that waxy starch required a longer relaxation time led to the hypothesis that also the aggregation formation rate might be slower with waxy starch compared to regular starch. Therefore the aggregation of SP+ and waxy starch was studied. By using waxy starch both the aggregate formation and the relaxation kinetics were monitored for the starch to SP+ particles charge ratio corresponding to maximum turbidity. The results are shown in Fig. 9. It can be seen that at short times the aggregates increased in size, going from the initial 22 nm in radius for the bare particles to three times that size after one minute, *i.e.* the aggregate formation is monitored. After approximately 5 minutes the aggregate size had reached a plateau of around 80 nm. With time, the size of the formed aggregates started to decrease due to relaxation of the starch chains. The aggregate size reaches a plateau again after approximately 500 minutes. This is in agreement with the turbidity measurements, where the turbidity change levels out after around the same period of time.

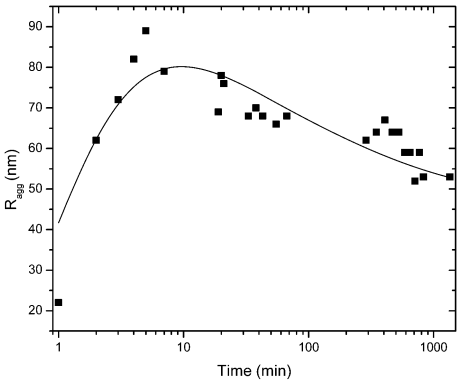

Fig. 9 Dynamic light scattering data where the aggregate size evolution is monitored with time for SP+ particles and waxy starch, at a particle to starch ratio corresponding to approximately 1 : 1 in charge ratio. The line is a guide for the eye.

The evolvement of the size distributions during the first 10 minutes after mixing reveals the formation of the aggregates at the initial step of aggregation and is shown in Fig. S6 (ESI†). At first, the primary particles still can be seen and the size distribution is bimodal. The peak corresponding to the primary particles decreases with time and the aggregate size increases. At the last time point relaxation takes place which can be seen by a decrease in aggregate size. The peak corresponding to the primary particles does not reappear during the relaxation, an observation in favour of rearrangement rather than singlet formation.

Conclusions

In this study the whole aggregation process, including aggregate formation, the transformation from electrostatic to steric stabilization and the relaxation kinetics, has been explored. In the investigation of aggregate formation the stability ratio, W, was determined and it was found that even at a starch to particle charge ratio of 1 the minimum W did not reach 1, which would have been an indication of a fully destabilized system. This was interpreted as the starch giving rise to steric stabilization at the 1 : 1 in charge ratio. At starch to particle ratios higher than 1 the electrophoretic mobility was reversed due to adsorption of the anionic starch and the values reached a plateau. However, the slightly net anionic charge of the complex at the plateau is not sufficient to provide stabilization *via* electrostatic repulsion. The steric contribution to stability from the highly branched, high molecular weight amylopectin fraction is significant.

The kinetics study also gives information about the aggregation mechanism. The initial, higher turbidity that could be seen

for the SP+ and starch mixture at the highest aggregation level, around the 1:1 in charge ratio, indicates that at first, the aggregates are larger, and the starch flocculates the particles more effectively *via* bridging flocculation. After rearrangement due to the electrostatic interaction between the polyelectrolyte and the oppositely charged particle surface the aggregation at equilibrium is due to patchwise flocculation. This means that a somewhat denser aggregate structure with smaller aggregate size is formed, which is manifested as a decrease in turbidity.

The two starch types, regular and waxy starch, gave rise to different turbidity intensities. The high molecular weight waxy starch induced a much higher initial turbidity. However, after relaxation the turbidity decreased for both starches and after sufficient time there was no longer a significant difference between them. A flocculation mechanism that goes from bridging flocculation, where the length of the polymer chain has a strong influence on the bridges formed, towards patchwise flocculation, which is more or less independent of the molecular weight of the polyelectrolyte, explains the initial difference between the starch types and also why there is no longer any difference after the equilibration state has been reached.

Acknowledgements

Financial support from the Swedish Research Council and the University of Geneva is gratefully acknowledged. The opportunity to go to MAX IV Laboratory for SAXS beam time is gratefully acknowledged. SuMo Biomaterials is gratefully acknowledged for providing economic and scientific support.

References

1 M. Borkovec and G. Papastavrou, *Curr. Opin. Colloid Interface Sci.*, 2008, **13**, 429–437.
2 A. Fuchs and E. Killmann, *Colloid Polym. Sci.*, 2001, **279**, 53–60.
3 J. Gregory, *J. Colloid Interface Sci.*, 1976, **55**, 35–44.
4 F. Mabire, R. Audebert and C. Quivoron, *J. Colloid Interface Sci.*, 1984, **97**, 120–136.
5 J. Zhang, C. Huguenard, C. Scarnecchia, R. Menghetti and J. Buffle, *Colloids Surf., A*, 1999, **151**, 49–63.
6 G. J. Fleer, T. Cosgrove, B. Vincent, M. A. Cohen Stuart and J. M. H. M. Scheutjens, *Polymers at interfaces*, Chapman & Hall, London, 1993.
7 A. A. Meier-Koll, C. C. Fleck and H. H. Von Grünberg, *J. Phys.: Condens. Matter*, 2004, **16**, 6041–6052.
8 S. Rosenfeldt, A. Wittemann, M. Ballauff, E. Breininger, J. Bolze and N. Dingenouts, *Phys. Rev. E: Stat., Nonlinear, Soft Matter Phys.*, 2004, **70**, 0614031.
9 K. Holmberg, B. Jönsson, B. Kronberg and B. Lindman, *Surfactants and polymers in aqueous solution*, Wiley, Chichester, 2003.
10 L. Feng, M. C. Stuart and Y. Adachi, *Adv. Colloid Interface Sci.*, 2015, **226**, 101–114.
11 I. Szilagyi, G. Trefalt, A. Tiraferri, P. Maroni and M. Borkovec, *Soft Matter*, 2014, **10**, 2479–2502.
12 T. W. Healy and V. K. La Mer, *J. Colloid Sci.*, 1964, **19**, 323–332.
13 J. Gregory, *J. Colloid Interface Sci.*, 1973, **42**, 448–456.
14 H. W. Walker and S. B. Grant, *Colloids Surf., A*, 1996, **119**, 229–239.
15 G. Gillies, W. Lin and M. Borkovec, *J. Phys. Chem. B*, 2007, **111**, 8626–8633.
16 Y. Shin, J. E. Roberts and M. M. Santore, *J. Colloid Interface Sci.*, 2002, **247**, 220–230.
17 K. Furusawa, M. Kanesaka and S. Yamashita, *J. Colloid Interface Sci.*, 1984, **99**, 341–348.
18 S. Schwarz, H. M. Buchhammer, K. Lunkwitz and H. J. Jacobasch, *Colloids Surf., A*, 1998, **140**, 377–384.
19 Y. Chen, S. Liu and G. Wang, *Chem. Eng. J.*, 2007, **133**, 325–333.
20 J. Gregory and I. Sheiham, *Br. Polym. J.*, 1974, **6**, 47–59.
21 R. J. Hunter, *Foundations of Colloid Science*, Oxford University Press, United States, 2001, ch. 12.8, pp. 616–617.
22 W. L. Yu, F. Bouyer and M. Borkovec, *J. Colloid Interface Sci.*, 2001, **241**, 392–399.
23 E. Seyrek, J. Hierrezuelo, A. Sadeghpour, I. Szilagyi and M. Borkovec, *Phys. Chem. Chem. Phys.*, 2011, **13**, 12716–12719.
24 J. Gregory and S. Barany, *Adv. Colloid Interface Sci.*, 2011, **169**, 1–12.
25 J. Gregory, *Colloids Surf.*, 1988, **31**, 231–253.
26 E. G. M. Pelssers, M. A. C. Stuart and G. J. Fleer, *Colloids Surf.*, 1989, **38**, 15–25.
27 Y. Adachi, *Adv. Colloid Interface Sci.*, 1995, **56**, 1–31.
28 R. Carceller and A. Juppo, *Pap. Puu*, 2004, **86**, 161–163.
29 F. Iselau, P. Restorp, M. Andersson and R. Bordes, *Colloids Surf., A*, 2015, **483**, 264–270.
30 K. Böckenhoff and W. R. Fischer, *Fresenius' J. Anal. Chem.*, 2001, **371**, 670–674.
31 R. Wäsche, M. Naito and V. A. Hackley, *Powder Technol.*, 2002, **123**, 275–281.
32 W. Brown, *Dynamic light scattering: the method and some applications*, Clarendon Press, Oxford, 1993.
33 T. Oncsik, G. Trefalt, M. Borkovec and I. Szilagyi, *Langmuir*, 2015, **31**, 3799–3807.
34 A. Labrador, Y. Cerenius, C. Svensson, K. Theodor and T. Plivelic, *J. Phys.: Conf. Ser.*, 2013, **425**, 072019.
35 J. Ilavsky, *J. Appl. Crystallogr.*, 2012, **45**, 324–328.
36 S. Chakraborty, B. Sahoo, I. Teraoka and R. A. Gross, *Carbohydr. Polym.*, 2005, **60**, 475–481.
37 K. Schätzel and J. Merz, *J. Chem. Phys.*, 1984, **81**, 2482–2488.
38 J. J. M. Swinkels, *Starch – Stärke*, 1985, **37**, 1–5.
39 F. Iselau, T. Phan Xuan, A. Matic, M. Persson, K. Holmberg and R. Bordes, *Soft Matter*, 2016, **12**, 3388–3397.
40 D. Kuakpetoon and Y. J. Wang, *Carbohydr. Res.*, 2006, **341**, 1896–1915.
41 J. A. De Witt and T. G. M. Van De Ven, *Langmuir*, 1992, **8**, 788–793.
42 R. Ferretti, J. Zhang and J. Buffle, *Colloids Surf., A*, 1997, **121**, 203–215.
43 L. C. E. Struik, *Physical Aging in Amorphous Polymers and Other Materials*, Elsevier, Amsterdam, 1978.

44 F. Alvarez, A. Alegra and J. Colmenero, *Phys. Rev. B: Condens. Matter Mater. Phys.*, 1991, **44**, 7306–7312.
45 S. L. Shamblin, B. C. Hancock, Y. Dupuis and M. J. Pikal, *J. Pharm. Sci.*, 2000, **89**, 417–427.
46 E. B. Stukalin, J. F. Douglas and K. F. Freed, *J. Chem. Phys.*, 2008, **129**, 094901.
47 S. Yoshioka, Y. Aso and S. Kojima, *Pharm. Res.*, 2001, **18**, 256–260.
48 S. A. H. R. S. Anderssen and R. J. Loy, *Anziam journal*, 2004, **45**, C800–C816.
49 R. M. Syamaladevi, G. V. Barbosa-Cánovas, S. J. Schmidt and S. S. Sablani, *Carbohydr. Polym.*, 2012, **88**, 223–231.
50 W. A. De Morais, M. R. Pereira and J. L. C. Fonseca, *Carbohydr. Polym.*, 2012, **87**, 2376–2380.
51 V. A. V. De Oliveira, W. A. De Morais, M. R. Pereira and J. L. C. Fonseca, *Eur. Polym. J.*, 2012, **48**, 1932–1939.
52 Y. Kawasaki, H. Watanabe and T. Uneyama, *Nihon Reoroji Gakkaishi*, 2011, **39**, 127–131.
53 Q. H. Yang, C. J. Qian, H. Li and M. B. Luo, *Phys. Chem. Chem. Phys.*, 2014, **16**, 23292–23300.
54 T. Cosgrove, T. L. Crowley, B. Vincent, K. G. Barnett and T. F. Tadros, *Faraday Symp. Chem. Soc.*, 1981, **16**, 101–108.